EFFECT OF WAKE STRUCTURE ON BLADE-VORTEX INTERACTION PHENOMENA: ACOUSTIC PREDICTION AND VALIDATION

Judith M. Gallman and Chee Tung
US Army Aeroflightdynamics Directorate, ATCOM
NASA Ames Research Center, Moffett Field, Ca., USA

Klaus-J. Schultz, Wolf Splettstoesser, and Heino Buchholz
Institut fur Entwurfsaerodynamik
Deutsche Forschungsanstalt fur Luft-und Raumfahrt
Braunschweig, Germany

Pierre Spiegel
Office National D'Etudes et de Recherches Aerospatiales
Chatillon, France

Casey L. Burley, Thomas F. Brooks, and D. Douglas Boyd, Jr.
NASA Langley Research Center, Hampton, Va., USA

ABSTRACT

During the Higher Harmonic Control Aeroacoustic Rotor Test, extensive measurements of the rotor aerodynamics, the far-field acoustics, the wake geometry and the blade motion for powered, descent, flight conditions were made. These measurements have been used to validate and improve the prediction of blade-vortex interaction (BVI) noise. The improvements made to the BVI modeling after the evaluation of the test data are discussed. The effects of these improvements on the acoustic-pressure predictions are shown. These improvements include re-structuring the wake, modifying the core size, incorporating the measured blade motion into the calculations and attempting to improve the dynamic blade response. A comparison of four different implementations of the Ffowcs Williams and Hawkings equation is presented. A common set of aerodynamic input has been used for this comparison.

1 INTRODUCTION

In order to correctly predict the aerodynamic and acoustic pressure for a helicopter operating in powered, descent flight, it is of utmost importance to correctly model the wake geometry of the vortices shed from the rotor tips. The wake-geometry model should contain information on the vortex location, the vortex strength and the vortex core size. In a recent, international cooperative test, Higher Harmonic Control (HHC) Aeroacoustic Rotor Test (HART), extensive measurements of the rotor aerodynamics, the far-field acoustics, the wake geometry, and the blade motions were made.[1] In preparation for this test, an international team of researchers from DLR, Germany, ONERA, France, the US Army Aeroflightdynamics Directorate (AFDD), and NASA Langley have been improving the prediction capability of blade vortex interaction (BVI) phenomena. This prediction capability includes models of the vortex geometry, aeroelastic blade motion, aerodynamic surface pressure, and far-field acoustic predictions.

The first validation effort of the prediction team was documented in Ref. 2. This validation effort included wake geometry predictions, aerodynamic surface pressure predictions and acoustic far-field predictions of the 2-bladed, 1/7 scale model OLS rotor tested in the Duits-Nederlandse Windtunnel (DNW) in 1982.[3,4] Leading edge pressure transducers at $x/c = 0.03$ and far-field acoustic data from this test were used for the validation efforts. The prediction codes compared reasonably well with the test data and captured the qualitative characteristics of the acoustic test data. However, further improvements to the wake geometry models are necessary to adequately predict the quantitative characteristics of the acoustic pressure needed to evaluate noise reduction techniques.

The second validation effort of the HART prediction team focused on the prediction of the wake geometry, aeroelastic blade motion, aerodynamic surface pressure, and far-field acoustics for the dynamically scaled, four-bladed, 40% model of the bearingless BO-105 main rotor.[5] The predictions are documented in Ref. 6. Unfortunately, only the far-field acoustic pressures were available for this validation effort. Therefore, the wake geometry, the aeroelastic and the aero-

 Presented at the First Joint CEAS/AIAA Aeroacoustic Conference (16th AIAA Aeroacoustic Conference, Munich, Germany, June 1995.

dynamic predictions of each prediction team member were compared to one another to provide a better understanding of how each method predicted the BVI phenomena. This exercise proved the importance of including the aeroelastic effects in the prediction of BVI noise. However, the most important conclusion of this exercise was that the prediction team needed to improve the modeling of the effect of 4/rev HHC on BVI noise for the BO105 model rotor.

The acoustic predictions of the third validation effort are documented in the current paper. The third validation effort is focused on predicting test points run during the HART program. The blades used for this test are the same BO105 model scale blades used for the European HELINOISE aeroacoustic rotor test.[7] Both the pre-test and the post-test acoustic predictions are presented. The pre-HART acoustic predictions are shown to indicate the status of the prediction ability before the HART data was available to help the prediction team improve their BVI phenomena modeling capability. The pre-HART predictions were done to help define the test matrix, improve the measurement techniques and to provide background for possible unexpected experimental results. A brief summary of the improvements made to the BVI modeling will also be included. For more information on the details of the improvements to the BVI modeling, see Ref. 8.

All the prediction team members use a numerical simulation of the Ffowcs Williams and Hawkings (FW-H) equation[9] to predict the acoustics. Therefore, all predictions require detailed information about the aerodynamic surface pressure on the rotor blade. The aerodynamic surface pressure calculations for the acoustic results shown in this paper are documented in Ref. 8. In order to directly compare the different implementations of the FW-H equation of each team member, a common set of blade surface pressures was used by all team members. These comparisons document any differences in acoustic predictions due to the different implementations of the FW-H equation.

2 THE ACOUSTIC PREDICTION CODES

For the acoustic calculations, the DLR has developed the acoustic code AKUROT,[10] ONERA computes the acoustics using the PARIS code[11], AFDD utilizes the RAPP code[12] and NASA Langley runs WOPWOP[13] to predict the acoustics. All the acoustic prediction codes use only the linear thickness and loading terms of the Ffowcs Williams and Hawkings equation, assuming that the noise from the nonlinear quadrupole term is negligible for the blade-vortex interactions studied in this program.

2.1 DLR Acoustic Prediction Methodology

To predict the acoustic pressure, the DLR uses the acoustic code AKUROT. This code was developed in 1987[4] and first validated with experimental data from the 1982 AH1-OLS model rotor test in the DNW. The code is based on Farassats formulation 1 derived from the FW-H equation and includes a thickness noise term and a loading noise term for the HART calculations.

The input data for the loading term are provided by the S4-rotor simulation code.[6] Since the aerodynamic model in the S4 code is based on lifting line theory, only sectional loading data is available at 20 radial stations and 180 azimuthal stations. For use in the acoustic prediction code, the loading data were interpolated to get inputs for 1024 azimuthal and 160 radial stations. The acoustic code uses a chordwise compact model of the loading noise.

2.2 NASA LaRC Acoustic Prediction Methodology

NASA Langley uses the rotor acoustic code WOPWOP[13] which implements the acoustic formulation 1A of Farassat to predict the acoustic pressure. The input to WOPWOP includes the physical characteristic of the rotor blade and the aerodynamic blade loading as a function of azimuthal position. For the predictions presented, the loads were input to WOPWOP every 1 degree of azimuth. When the aerodynamic input used in WOPWOP is calculated by HIRES[14], the loading noise is modeled by a chordwise compact source. When a chordwise distribution of the blade loading is available from the full potential code FPRBVI, the loading noise is modeled by noncompact sources distributed over the chord.

2.3 ONERA Acoustic Prediction Methodology

At ONERA, the noise radiation is computed by the PARIS code[11] using a pressure distribution provided by ARHIS.[11] The azimuthal step size of the input data depends on the impulsivity of the interactions. An efficient spanwise interpolation model has been implemented in PARIS in order to minimize the amount of airload data required for BVI noise predictions. This interpolation method identifies the BVI impulsive events in the acoustic signatures generated at each individual blade section and accounts for their phase and amplitude. This method, used with aerodynamic data from 10 blade sections, provides the same result as a prediciton without interpolation that uses airload data from 30 blade sections. PARIS provides the correlation between the peaks of a BVI noise signature and the corresponding source locations on the rotor disk.

2.4 AFDD Acoustic Prediction Methodology

At AFDD, RAPP[12], a rotor acoustic prediction program based on the FW-H equation, calculates the acoustic pressure using the FPR[15–18] computed surface pressures. RAPP can use either the chordwise compact or noncompact formulation. When the force

terms in the FW-H equation are modeled as chordwise compact sources, the sources are distributed spanwise along the quarter chord of the acoustic planform. The acoustic planform consists of the locations of the contributing sources. This method is referred to as the acoustic lifting line method.

When the noncompact formulation is used to model the force terms, 20 sources are distributed over the airfoil surface at each spanwise location. For both formulations, 11 spanwise stations, distributed over the outer 60% of the span, are used in the computation. The time step for the acoustic calculation is 0.7 degrees. The time resolution of the input aerodynamic loading is 0.125 degrees. The advantage of the compact formulation as compared to the noncompact formulation is the reduced time and memory required. For the compact formulation, only the section loading is needed at each spanwise location for each time step (0.125 degrees). Whereas, for the noncompact formulation, the pressure at the 20 surface points is needed at each spanwise station for each time step.

3 TEST AND MODEL DESCRIPTION

The HHC aeroacoustic rotor test configuration consisted of a Mach scaled, 40% model of the hingeless BO105 main rotor mounted on the DLR test rig. The rectangular rotor blades have -8 degrees of linear twist, a radius of 2 meters, a constant chord of 0.121 meters and a modified NACA 23012 airfoil. The model is highly instrumented with 124 pressure transducers and 53 strain gages. The test was run in the 6m x 8m open jet configuration of the DNW. The acoustic measurements were made with an array of eleven microphones mounted on a ground based traverse mechanism. The microphones are arranged symmetrically with respect to the rotor hub and are spaced 0.54 meters apart. The traverse, located 2.3 meters below the hub of the rotor, travels from 4 meters upstream of the rotor hub to 4 meters downstream of the rotor hub. Data is acquired while the microphone array is continuously traversing downstream, but the actual measurement locations are at 0.5 meter intervals starting at 4.0 meters upstream of the hub resulting in 187 measurement locations below the rotor hub. Figure 1 shows the resulting grid of measurement locations with respect to the rotor plane. One microphone was located on the body of the test rig and two microphones were mounted in the plane of the rotor on the 8m x 6m nozzle. For each test condition, the acoustic pressure was recorded for 30 rotor revolutions at a rate of 2048 data points per revolution. The pressure time histories and sound pressure level contours presented in this paper for code validation are based on an ensemble average of 30 revolutions.

The HART test matrix consisted of descent flight conditions with a variation of the glide path angle from -3 degrees to +12 degrees and a variation of the advance ratio from 0.144 to 0.275. The nominal test condition, or the baseline case, simulated a landing approach with

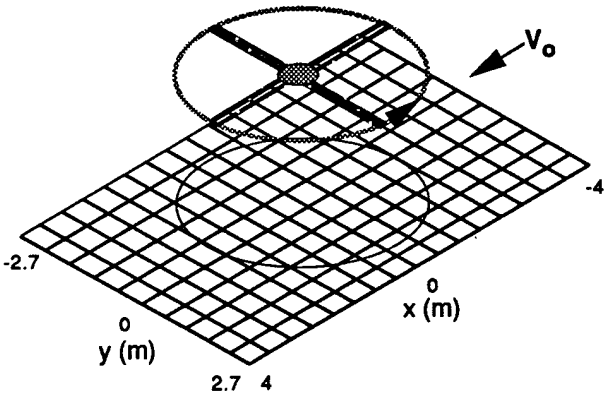

Fig. 1 Grid of 187 microphone locations below the rotor plane.

a glide path angle of 6 degrees and an advance ratio, μ, of 0.15. This case corresponds to a shaft tilt angle, α_s, of 5.3 degrees and a wind tunnel velocity of 33 meters/second. For this baseline condition, a systematic variation in phase shift of the HHC was performed for 3-,4- and 5/rev input of 0.8 degree amplitude. The most effective HHC input for reducing noise and vibrations was the 3/rev. Therefore, the measured data and the analytic solutions presented in this paper for code validation will be the baseline case and 2 cases with 3/rev HHC input of 0.8 degrees. One case corresponds to low noise and one case corresponds to low vibrations. The test conditions presented in this paper are listed in Table 1.

4 RESULTS

For the test cases listed in Table 1, the measured and predicted acoustic pressure time histories are presented at the location of maximum, mid-frequency, sound pressure level (SPL) on the retreating side and on the advancing side of the rotor. The locations of maximum, mid-frequency, SPL are different for each test condition and are listed in Table 2. The average time history at each measurement point below the rotor (see Fig. 1) is used to determine the mid-frequency SPL. The band limit is the 6th to the 40th blade passage frequency. This mid-frequency band is believed to contain the frequencies present in BVI noise. The measured, mid-frequency, SPL contour plots for the three test cases listed in Table 1 are shown in Fig. 2. The measured, acoustic-pressure time histories are shown in Fig. 3 at the maximum SPL locations listed in Table 2. Please note that in normalized time, one rotor revolution is equal to one unit of time.

The pre-test and post-test acoustic predictions (acoustic-pressure time histories and mid-frequency, SPL contours) from each research center are presented in the following sections to indicate which improvements to the BVI prediction methodology have the greatest potential. A brief description of the changes made to the BVI prediction methodology by each re-

	C_T	μ	α_s (deg)	RPM	HHC amp (deg)	HHC phase (deg)
Baseline (Run 140)	0.00432	0.152	5.3	1041	0.0	0.0
Low Noise (Run 138)	0.00413	0.152	5.3	1041	0.87	296
Low Vibration (Run 133)	0.0044	0.151	5.3	1041	0.83	177

Table 1 Test points used for code validation

	advancing side			retreating side		
	x (m)	y (m)	z (m)	x (m)	y (m)	z (m)
Baseline (Run 140)	0.0	2.18	-2.29	2.0	-1.07	-2.28
Low Noise (Run 138)	-0.5	1.1	-2.29	2.0	-1.07	-2.28
Low Vibration (Run 133)	0.05	2.18	-2.29	2.5	-1.07	-2.28

Table 2 Microphone positions for maximum SPL

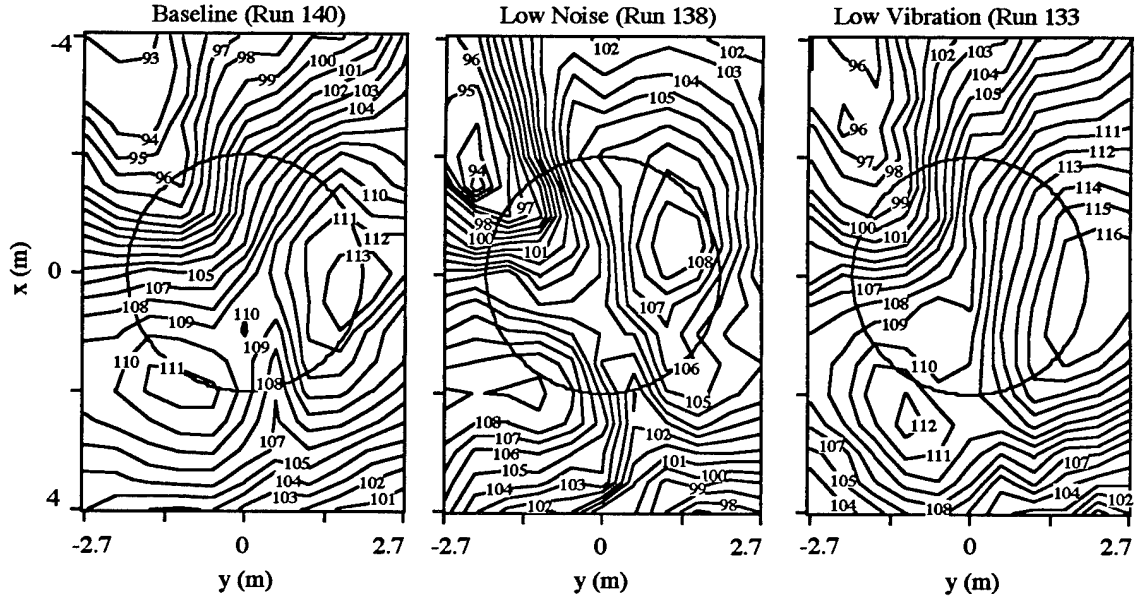

Fig. 2 Measured, mid-frequency (6th-40th harmonic), SPL contour plots for the test cases listed in Table 1.

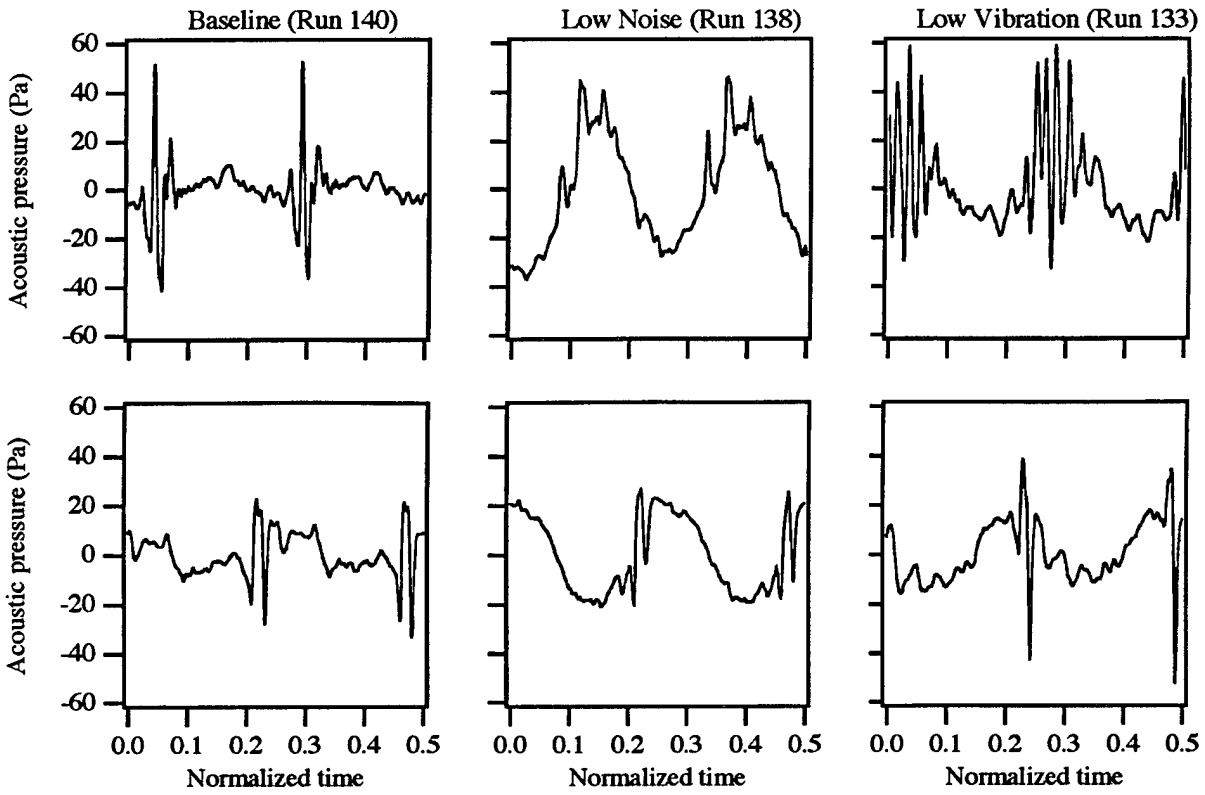

Fig. 3 Measured, acoustic-pressure time histories for the test cases listed in Table 1. Row 1) advancing side microphone locations listed in Table 2. Row 2) retreating side microphone locations listed in Table 2.

search center is included.

4.1 DLR Pre-HART and Post-HART Acoustic Predictions

The pre-HART acoustic predictions made by the DLR are based on spanwise blade loadings provided by the S4 rotor simulation code described in Ref. 6. For the post-HART acoustic predictions, the wake model in S4 has been modified. The modification to the wake model is mainly an application of a wake contraction model. A 15% contraction has been applied to the to the baseline case and low noise case and a 10% contraction has been applied to the low vibration case. Also, the vortex core radius was redefined to be equal to the vortex core measured during the HART program. In an attempt to determine the effect of wake geometry on the aeroacoustic predictions for the two cases with HHC, the orientation of the wake with respect to the tip path plane was adjusted so that the miss distance between the blade and the vortex would be similar to the measurements made of the miss distance during the HART program. In addition for the low vibration case, a double vortex structure was used as measured during the HART test. The predicted, acoustic-pressure time histories for the three test cases at the advancing-side microphone locations listed in Table 2 are shown in Fig. 4. The retreating-side microphones are shown in Fig. 5. The top row contains the pre-test predictions and the bottom row contains the post-test predictions. For the baseline case, the wake re-structuring improves the peak-to-peak levels of the wave form on the advancing side. Not only is the peak-to-peak level improved on the advancing side for the low noise case, but the overall wave form compares better to the measured data. The changes to the wave forms due to the wake re-structuring do not improve the predictions for the low vibration case. Perhaps the wake re-structureing needs to be optimized for each test case. The contour plots of the mid-frequency SPLs for the three test cases are shown in Fig. 6. The contour plots in the first row are the pre-HART predictions and the contour plots in the second row are the post-HART predictions. The wake re-structuring only slightly affects the contour plots for the baseline case. However, it improves both the magnitude and the directivity characteristics of the low noise and the low vibration cases.

4.2 NASA LaRC Pre-HART and Post-HART Acoustic Predictions

The methodology used to predict the spanwise blade loading for the pre-HART acoustic predictions made by NASA LaRC is also discussed in detail in Ref. 6. The prediction method begins with a 10 degree

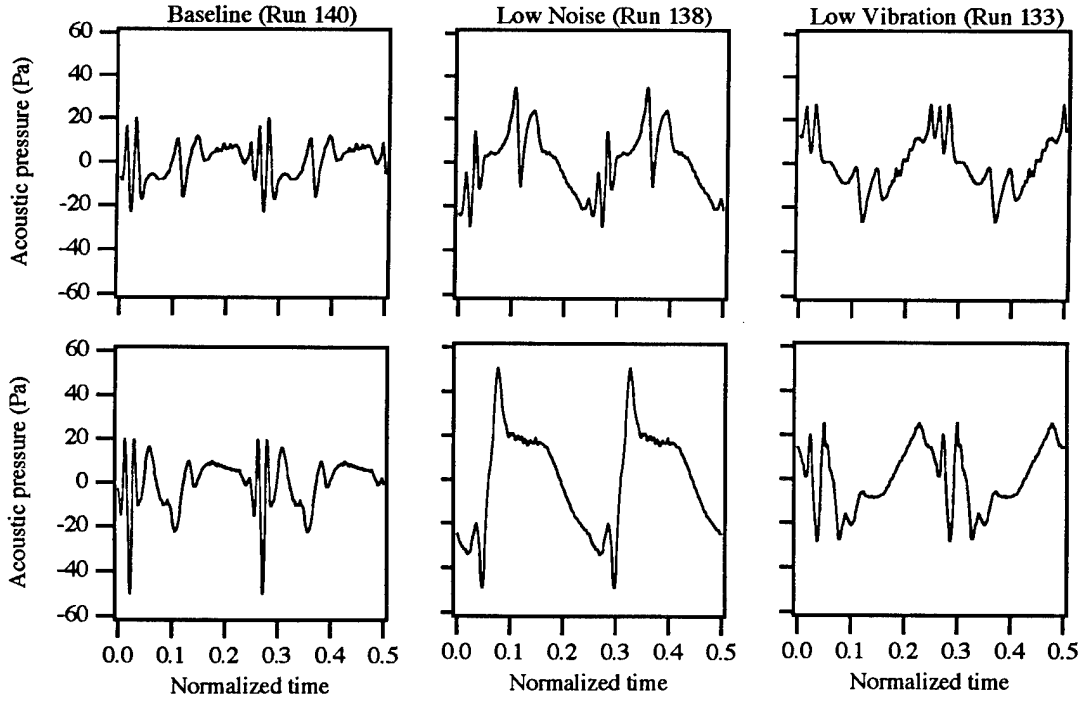

Fig. 4 DLR predicted, acoustic-pressure time histories for the advancing side microphone locations listed in Table 2. Row 1) pre-test predictions. Row 2) post-test predictions.

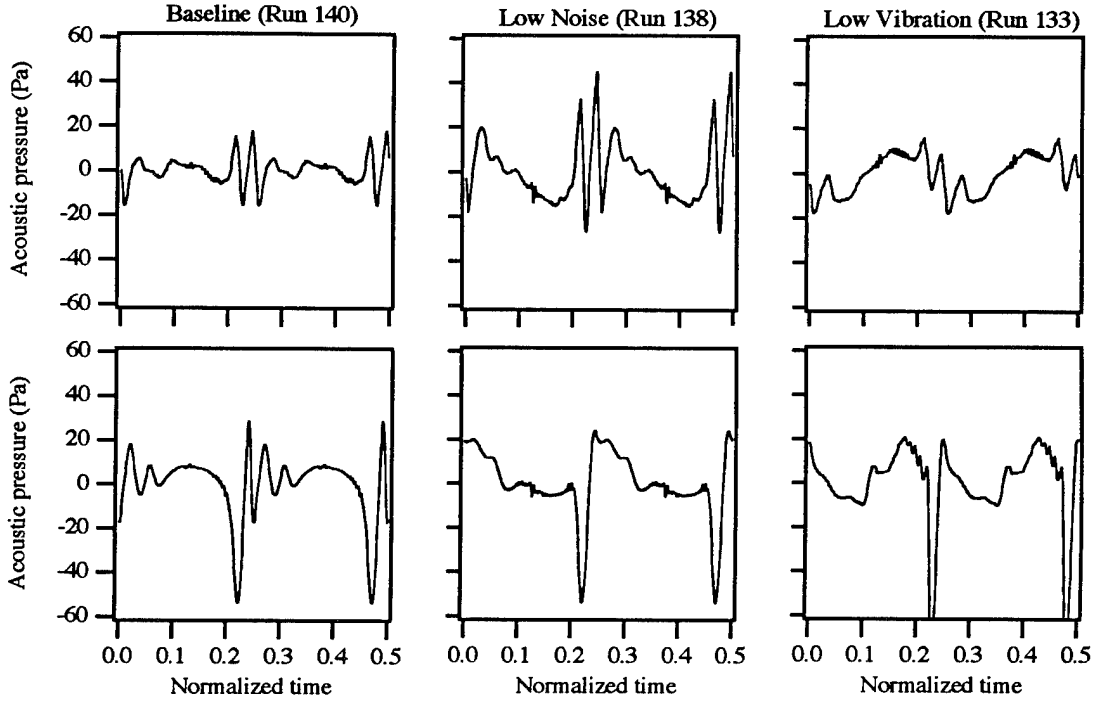

Fig. 5 DLR predicted, acoustic-pressure time histories for the retreating side microphone locations listed in Table 2. Row 1) pre-test predictions. Row 2) post-test predictions.

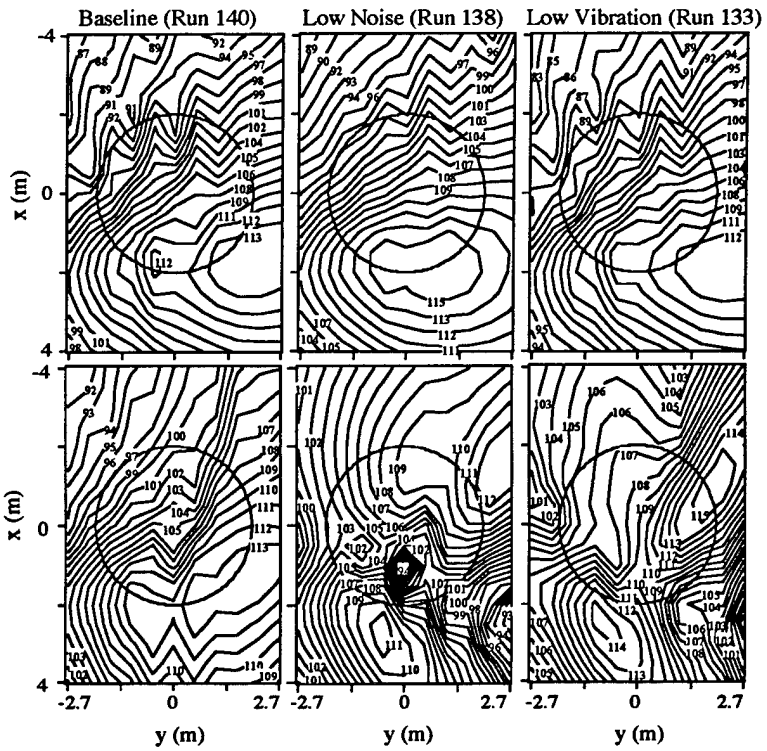

Fig. 6 DLR predicted, mid-frequency, SPL contours. Row 1) pre-test predictions. Row 2) post-test predicitons.

azimuthal resolution of the rotor wake calculated by CAMRAD.Mod1. HIRES then computes the airloads at 1 degree azimuthal increments and at 75 radial stations. The rotor blade dynamics are calculated by CAMRAD.Mod1. For the post-HART predictions, the measured blade dynamics are used to prescribe the blade motion in CAMRAD.Mod1 before the HIRES computation of the airloads. The NASA LaRC predicted, acoustic-pressure time histories at the advancing-side microphone locations for the three test cases are shown in Fig. 7. The retreating-side microphone locations are shown in Fig 8. The time histories in the top row are the pre-test predictions and the time histories in the bottom row are the post test predictions. The peak-to-peak levels are reduced on the retreating side of the rotor for the baseline case when the measured blade dynamics are used for the prediction, but the waveform does not change. For the low noise case, the low frequency character of the waveform is increased and the peak-to-peak levels are decreased by the application of the measured blade dynamics. The low vibration case is similar to the baseline case, wherein the peak to peak levels are reduced on the retreating side without much change to the waveform when the predicted blade dynamics are replaced by the measured blade dynamics in the prediction of the airloads. The pre-test and post-test, LaRC-predicted contour plots of the mid-frequency SPLs are shown in Fig. 9. For the baseline case, the SPLs are reduced in the post-test calculations. Also, the local peak on the retreating side has been eliminated. The elimination of the local peak in the post-test prediction is also evident for the low noise case. For this case, the levels over the whole contour have been decreased. The low vibration case changes only slightly by the application of the measured blade motion to the airloads prediction. The peak levels on the retreating side are reduced without the elimination of the retreating side local maximum.

4.3 ONERA Pre-HART and Post-HART Acoustic Predictions

A detailed description of the pre-test ONERA prediction methodology can be found in Ref. 6. The prediction methodology consists of a vortex sheet roll-up model that results in interacting vortices.[19] For the pre-HART predictions, the viscous vortex core radius in ARHIS was determined by an evolution law based on extrapolated hot-wire measurements of a two-bladed rotor model in hover.[20] The viscous core radii obtained with this law are often smaller than 0.1 chord on the advancing side and approximately 0.15 on the retreating side. The post-test AHRIS vortex core size model uses an improved evolution law based on the preliminary analysis of the HART LDV measurements. The adjusted law results in viscous core radii of 0.25 chords on the retreating side that are in

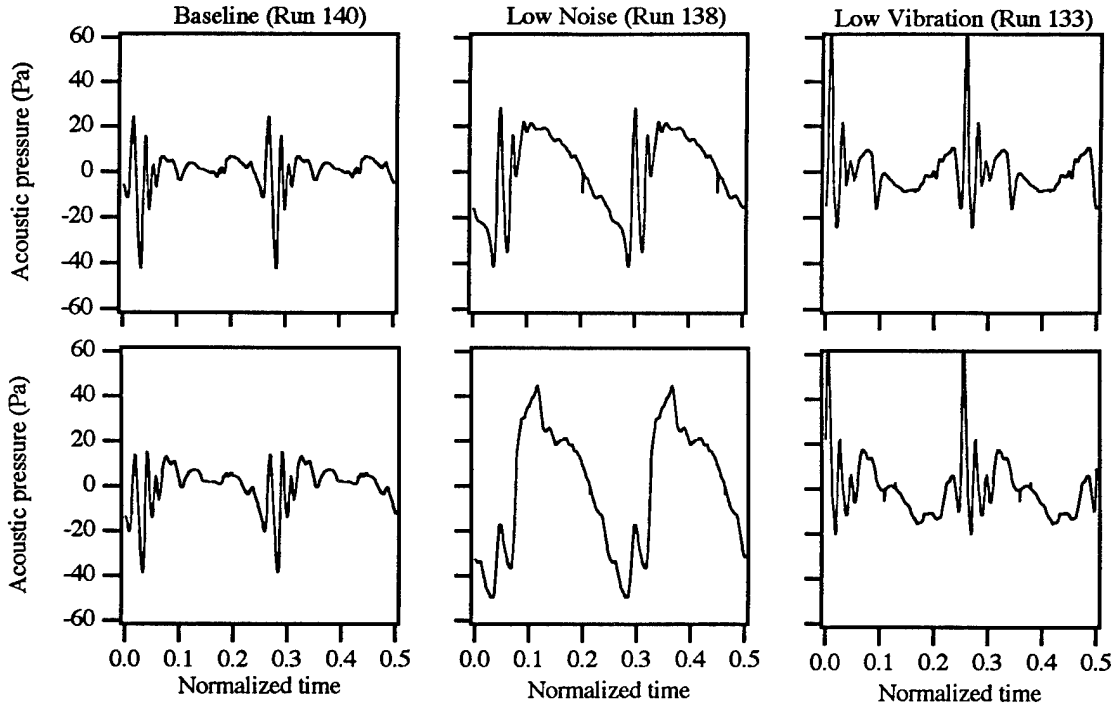

Fig. 7 NASA LaRC predicted, acoustic-pressure time histories for the advancing side microphone locations listed in Table 2. Row 1) pre-test predictions. Row 2) post-test predictions.

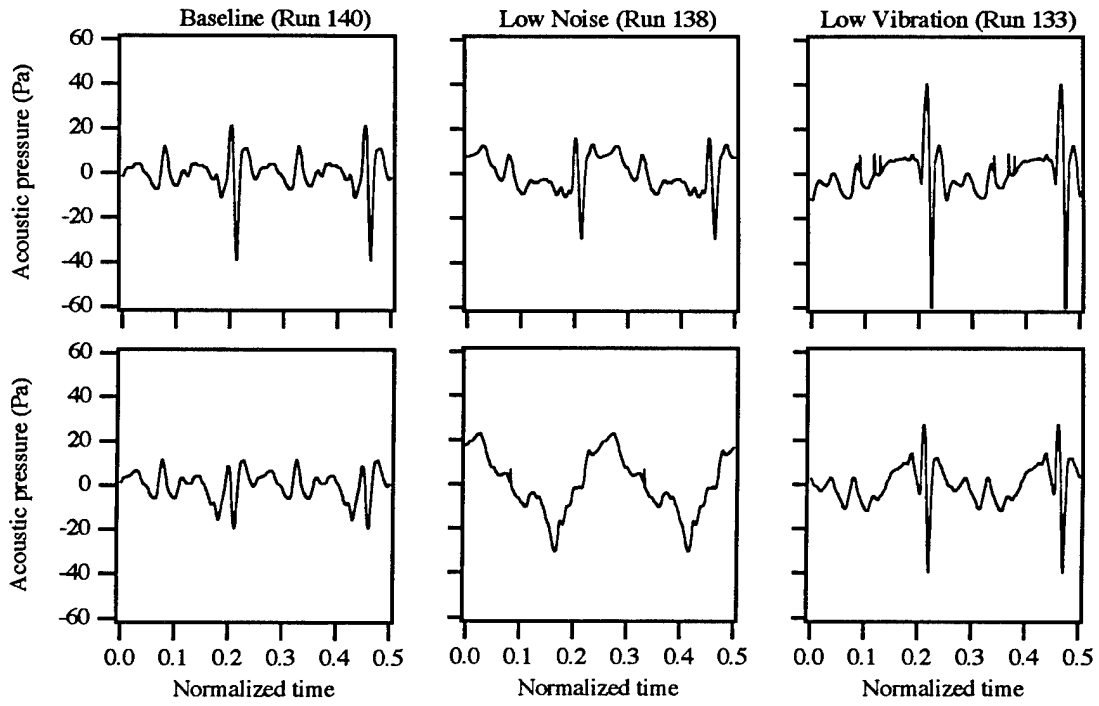

Fig. 8 NASA LaRC predicted, acoustic-pressure time histories for the retreating side microphone locations listed in Table 2. Row 1) pre-test predictions. Row 2) post-test predictions.

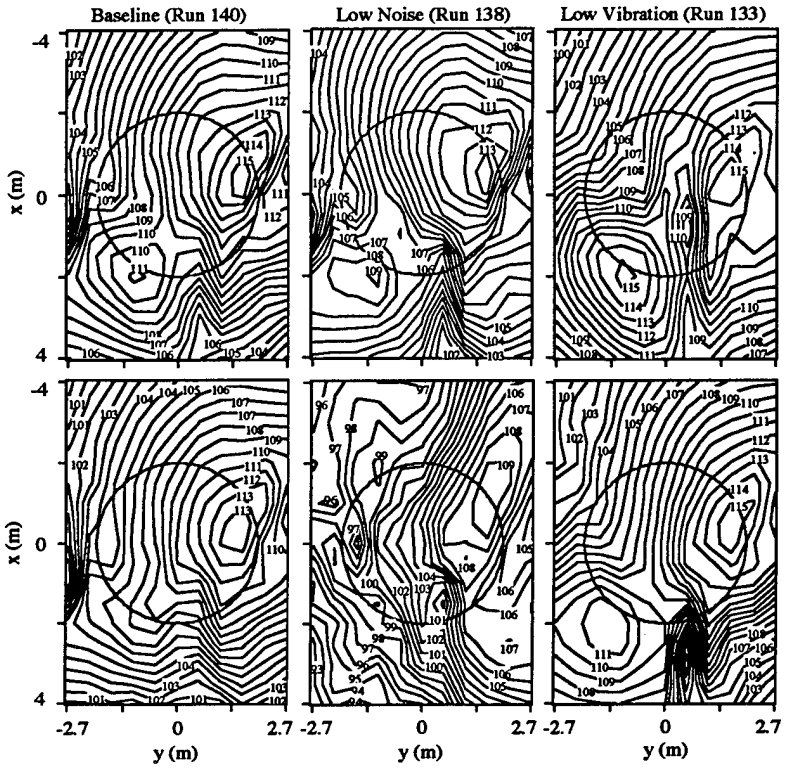

Fig. 9 NASA LaRC predicted, mid-frequency, SPL contours. Row 1) pre-test predictions. Row 2) post-test predicitons.

agreement with the experimental data. The viscous core radii on the advancing side only changes slightly. The ONERA predicted, acoustic-pressure time histories of the three test cases are shown in Fig. 10 for the advancing side microphone locations. The retreating side microphone locations are shown in Fig. 11. The only difference between the pre-HART (top row) and the post-HART (bottom row) acoustic-pressure time histories for all three test cases is the magnitude of the peaks. This is the expected result of increasing the core radius in the airloads computation. The ONERA predicted, pre-test and post-test, mid-frequency SPLs are shown in Fig. 12. The only difference between the pre-test and post-test SPL contours are the lower levels for the post-test predictions.

4.4 AFDD Pre-HART and Post-HART Acoustic Predictions

The main differences between the pre-HART predictions and the post-HART predictions made by AFDD are a change to the partial angle calculation and the fine tuning of the dynamic model of the rotor blade in an attempt to improve the dynamic blade motion. The AFDD pre-HART prediction methodology is summarized in Ref. 6. A closer look at the partial angles calculated by CAMRAD/JA revealed that the angles were not being calculated correctly. CAMRAD/JA computes the partial angles by subtracting the induced velocity caused by the tip vortices within the computational domain of FPR from the inflow angles. Specifying a core radius of 2.0 chords for the partial angle calculation eliminates the anomalies from the partial angle calculation. A core radius of 0.20 chords is used for all other CAMRAD/JA and FPR calculations. The AFDD predicted, acoustic-pressure time histories of the three test cases are shown in Fig. 13 for the advancing-side microphone locations. The predicted acoustic pressure for the retreating-side microphone locations are shown in Fig. 14. There is only a slight change in magnitude between the pre-test and post-test predictions without much change in waveform for both the advancing and retreating side microphone locations. The AFDD predicted, mid-frequency, SPL contours are shown in Fig. 15. There is little difference between the pre-test and post-test prediction of the SPLs for the baseline case. The slight decrease in contour levels for this case is most likely caused by the change in the partial angles. The contour levels for the low noise case actually increase for the post-HART predictions with only a slight change in directivity. The actual contour levels for the low vibration case change only slightly, but the local maximum on the advancing side has moved aft for the post-test predictions.

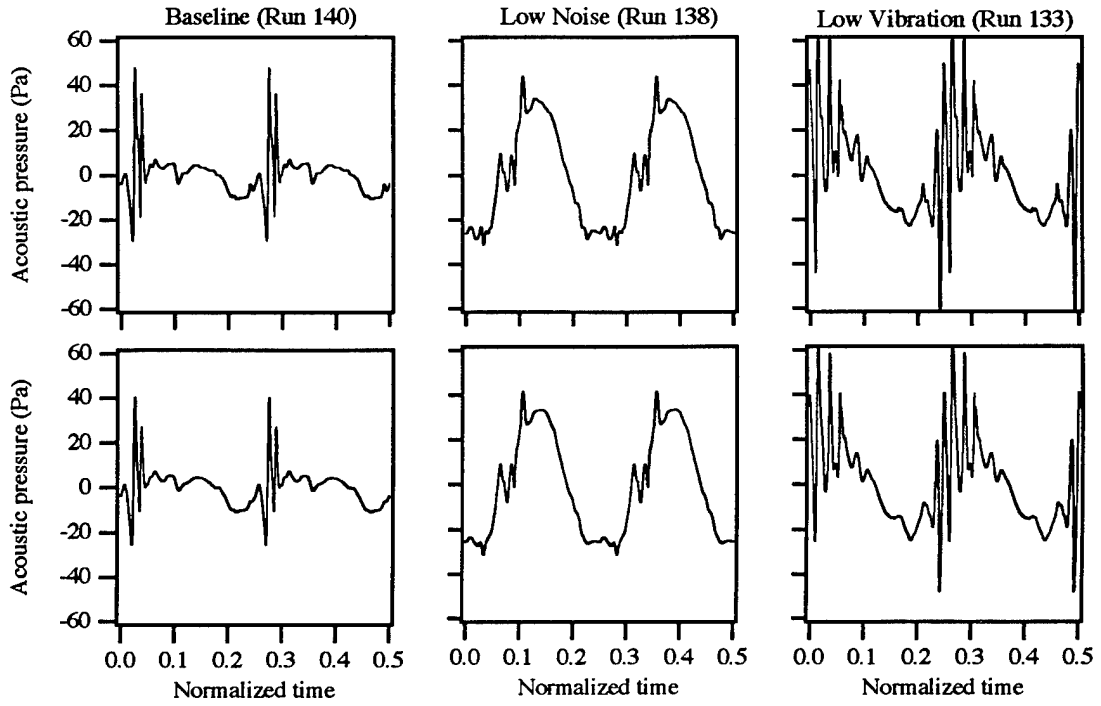

Fig. 10 ONERA predicted, acoustic-pressure time histories for the advancing side microphone locations listed in Table 2. Row 1) pre-test predictions. Row 2) post-test predictions.

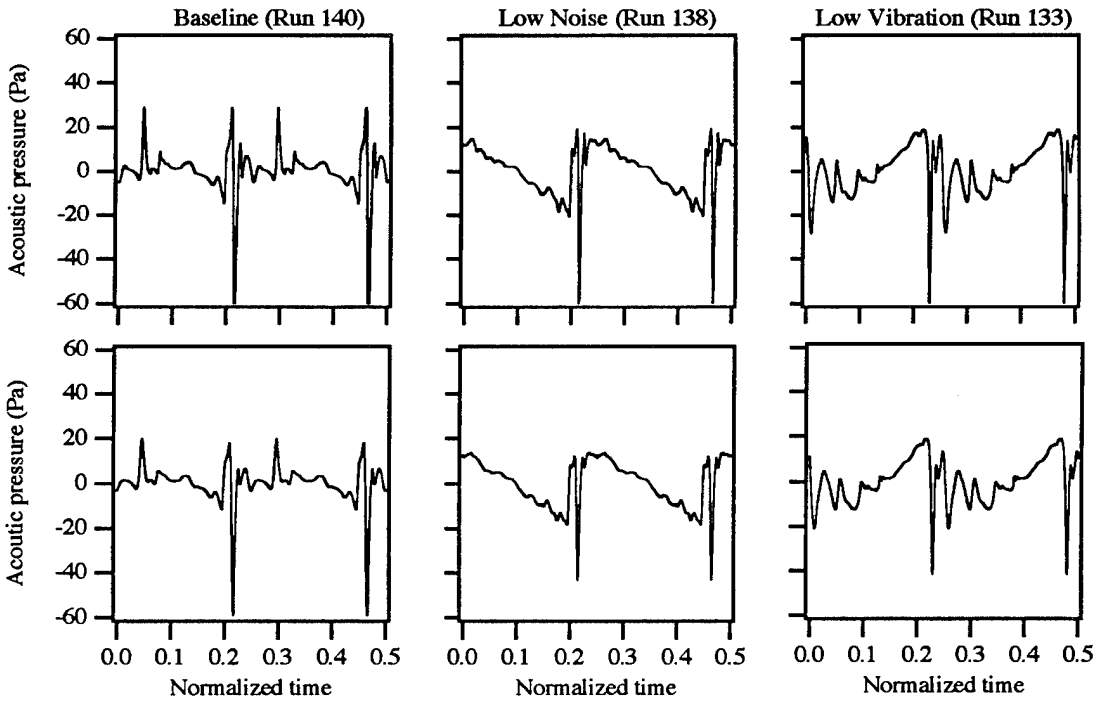

Fig. 11 ONERA predicted, acoustic-pressure time histories for the retreating side microphone locations listed in Table 2. Row 1) pre-test predictions. Row 2) post-test predictions.

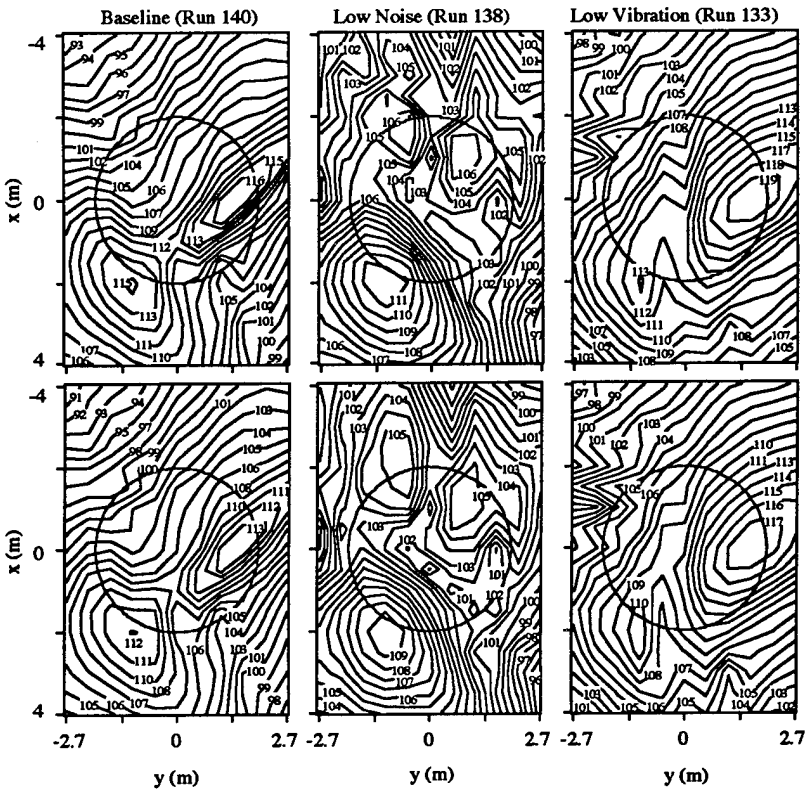

Fig. 12 ONERA predicted, mid-frequency, SPL contours. Row 1) pre-test predictions. Row 2) post-test predicitons.

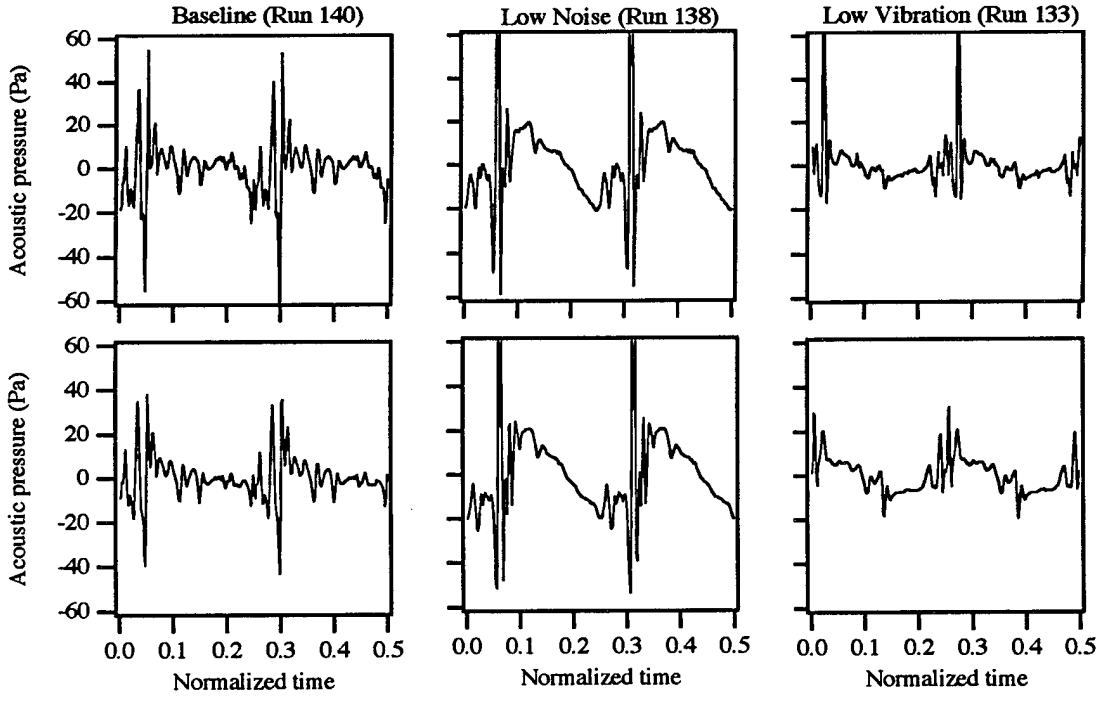

Fig. 13 AFDD predicted, acoustic-pressure time histories for the advancing side microphone locations listed in Table 2. Row 1) pre-test predictions. Row 2) post-test predictions.

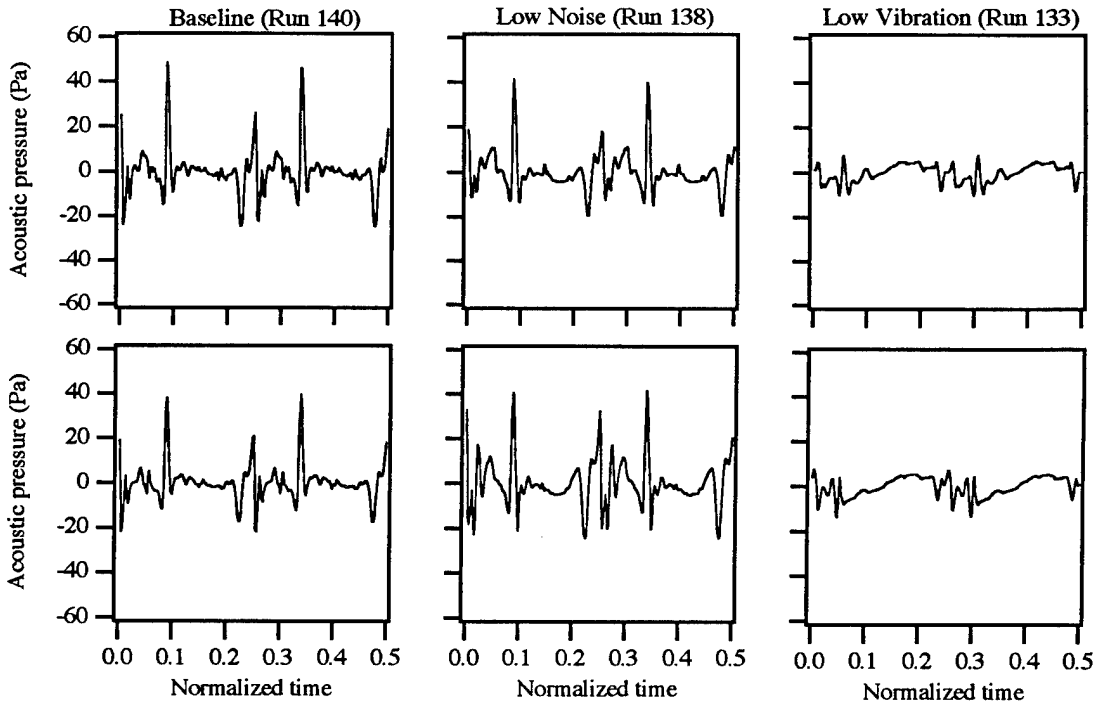

Fig. 14 AFDD predicted, acoustic-pressure time histories for the retreating side microphone locations listed in Table 2. Row 1) pre-test predictions. Row 2) post-test predictions.

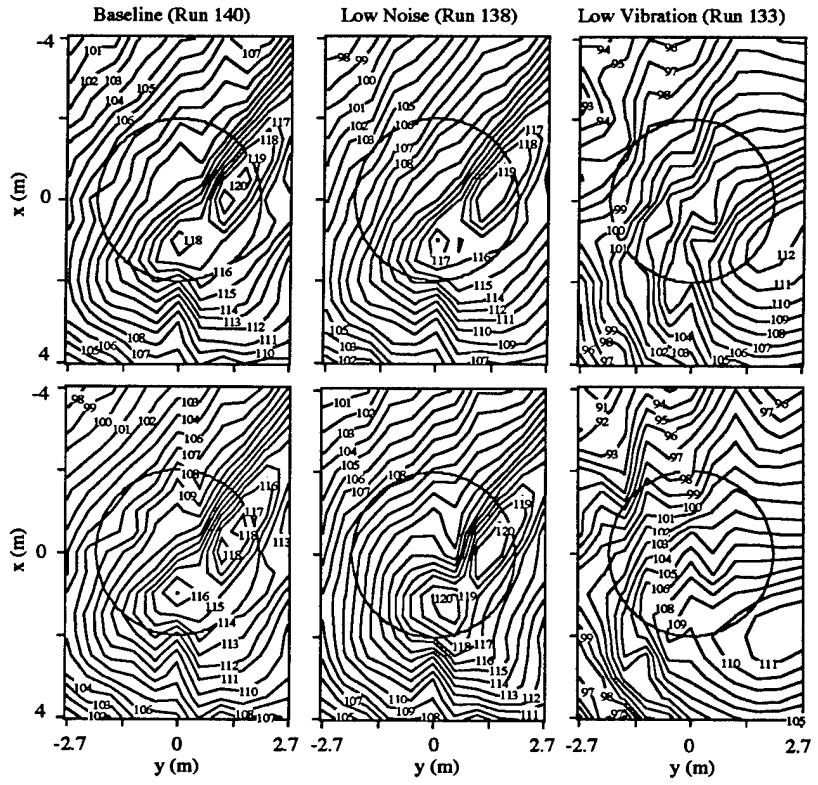

Fig. 15 AFDD predicted, mid-frequency, SPL contours. Row 1) pre-test predictions. Row 2) post-test predicitons.

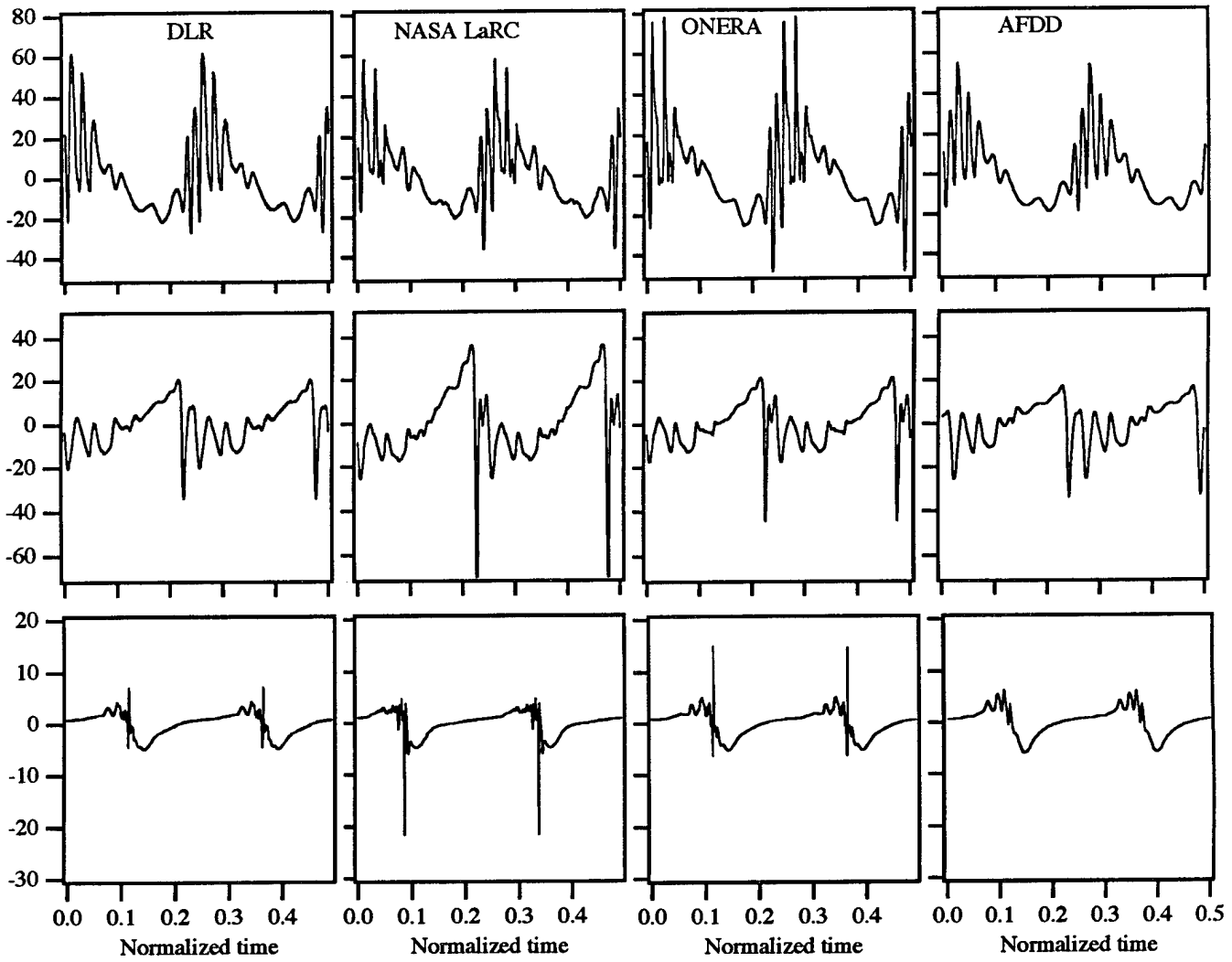

Fig. 16 Predicted, acoustic-pressure time histories using a common set of aerodynamic input for Run 133. Row 1) advancing side microphone location listed in Table 2 for Run 133. Row 2) retreating side microphone location listed in Table 2 for Run 133. Row 3) in-plane microphone location.

5 ACOUSTIC PREDICTIONS USING COMMON AERODYNAMIC INPUT

Even though all the prediction team members use a numerical simulation of the Ffowcs Williams and Hawkings equation, each implementation is different. To determine if there are any differences in the acoustic predictions caused by the specific implementations of the FW-H equation, all the prediction team members used a common set of aerodynamic blade surface pressures. The common set is a prediction of the low vibration case (Run 133) provided by ONERA. Each team member used the blade loading at the same 30 radial stations and 41 chordwise positions for the non-compact model of the dipole source. All acoustic predictions for this case were made assuming that the rotor was stiff, i.e. no flapping, bending or torsion. The measured cyclic and collective pitch were used to determine the blade attitude. Also, the uncorrected shaft angle was used to define the location of the blade with respect to the observer. The resulting predicted, acoustic-pressure time histories are shown in Fig. 16 for the advancing and retreating side microphone locations in Table 2 for Run 133 and for a microphone located in the plane of the rotor. This in-plane microphone is mounted on the nozzle and is at x = -6.71 m, y = 3.395 m, and z = 0.0. There are only a few slight differences in magnitude for the acoustic predictions at the advancing side microphone. The differences in magnitude are much greater for the predictions at the retreating side microphone. For the predictions at the inplane microphone, the main difference is the magnitude of the spike and the fact that it is not evident in the AFDD predictions. The predicted, mid-frequency, SPL contours are shown in Fig. 17. The character of the directivity pattern is quite similar for all four

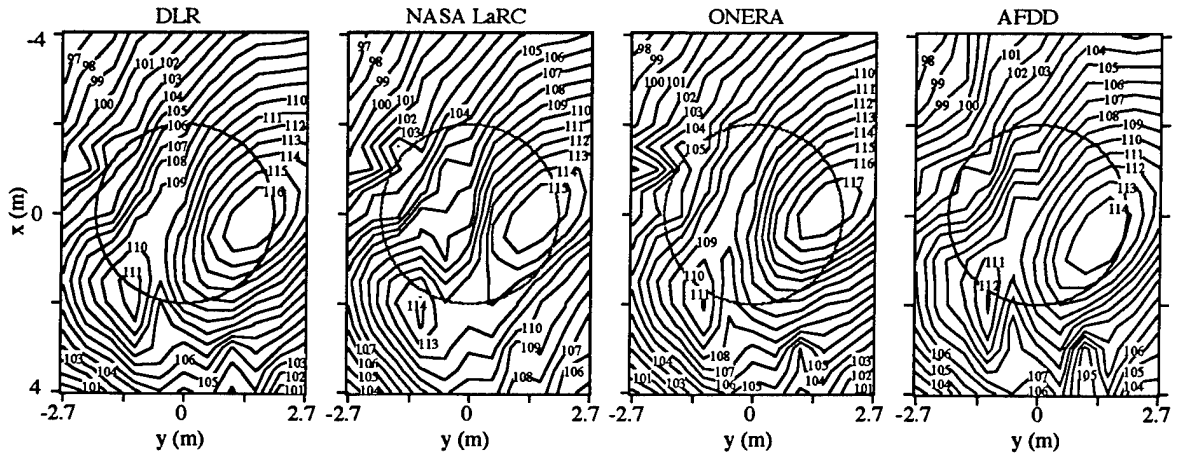

Fig. 17 Predicted, mid-frequency, SPL contours for Run 133, using a common set of aerodynamic input.

methods. NASA LaRC predicts higher levels downstream of the rotor than do the rest of the prediction team, and the local maximum on the advancing side is slightly higher for the ONERA predictions.

6 SUMMARY AND CONCLUSIONS

The pre-test and post-test acoustic predictions for the Higher Harmonic Control Aeroacoustic Rotor Test have been presented. The comparisons between the pre-test and post-test predictions indicate how the HART program can guide researchers to improve the aeroacoustic and dynamic modeling of the BVI phenomena so that low noise concepts such as HHC can be explored. To improve their prediction capability, the DLR combined a contraction of their prescribed wake model with a re-orientation of the wake geometry with respect to the tip path plane. This re-structuring of the wake can improve the aeroacoustic predictions and will be used to refine the DLR free-wake model. The substitution of the measured blade dynamics for the predicted dynamics does improve the aeroacoustic predictions made by NASA LaRC. This example demonstrates the necessity of properly calculating the blade motion for BVI noise predictions, especially for cases with HHC input. ONERA's post-test predictions show that changing the core size of the interacting vortices to more closely agree with the measured core sizes improves the prediction of the magnitude of the predicted, acoustic-pressure time histories and the SPL contours. AFDD's fine tuning of the dynamic model of the rotor blade affected the aeroacoustic predictions only slightly. The prediction of the dynamic blade motion by CAMRAD/JA is still not adequate for the cases with HHC input.

There are distinct differences in the acoustic predictions made by each of the prediction team members when the same aerodynamic input is used. The exact cause of these difference is not currently obvious, but documenting the extent of the differences should help the rotorcraft community understand where the state-of-the-art lies in acoustic prediction methodology.

ACKNOWLEDGEMENTS

The authors would like to thank the HART test team for their efforts that resulted in a successful test and for making the HART data available for the improvement of the BVI prediction methodology.

REFERENCES

[1]Yu, Y.H., Gmelin, B., Heller, H., Phillipe, J.J., Mercker, E., and Preisser, J.S., "HHC Aeroacoustics Rotor Test at the DNW-The Joint German/French/US HART Project," Twentieth European Rotorcraft Forum, Amsterdam, The Netherlands, Oct. 1994.

[2]Yu, Y.H., Tung, C., Gallman, J.M., Splettstoesser, W.R., Schultz, K.J., van der Wall, B., Spiegel, P., and Rahier, G., "Aerodynamics and Acoustics of Rotor Blade-Vortex Interactions: Analysis Capability and Its Validation," AIAA 93-4332, 15th AIAA Aeroacoustic Conference, Long Beach, Ca, Oct. 1993.

[3]Boxwell, D.A., Schmitz, F.H., Splettstoesser, W.R., and Schultz, K.J, "Model Helicopter Rotor High-Speed Impulsive Noise: Measured Acoustics and Blade Pressures," Ninth European Rotorcraft Forum, Stresa, Italy, Sept. 1983.

[4]Boxwell, D.A., Schmitz, F.H., Splettstoesser, W.R., and Schultz, K.J, "Helicopter Model Rotor-Blade Vortex Interaction Impulsive Noise: Scalability,

and Parametric Variations," *Journal of the American Helicopter Society*, Vol. 32, No. 1, Jan. 1987.

[5]Splettstoesser, W.R, Schultz, K.J., Kube, R, Brooks, T.F., Booth, E.R., Neisl, G., and Streby, O., "BVI Impulsive Noise Reduction by Higher Harmonic Pitch Control: Results of a Scaled Model Rotor Experiment in the DNW,"Seventeenth European Rotorcraft Forum, Berlin, Germany, Sept. 1991.

[6]Beaumier, P., Prieur, J., Rahier, G., Spiegel, P., Demargne, A., Kube, R., van der Wall, B.G., Schultz, K.J., Splettstoesser, W.R., Tung, C., Gallman, J.M., Yu, Y.H., Brooks, T.F., Burley, C.L., and Boyd, D.D., "Aerodynamic and Acoustic Effect of Higher Harmonic Control on Helicopter Rotor Blade-Vortex Interaction: Predictions and Preliminary Validations," 75th Fluid Dynamics Panel Meeting and Symposium on Aerodynamics and Aeroacoustics of Rotorcraft, AGARD, Berlin Germany, Oct., 1994.

[7]Sploettstoesser, W.R., Niesl, G. Cenedese, F. Nittie, F. and Papanikas, D.G., "Experimental Results of the European HELINOISE Aeroacoustic Rotor Test in the DNW," *Proceedings of the 19th European Rotorcraft Forum*, paper no. B8, Sept. 1993, Cernobbio, Italy.

[8]Tung, C., Gallman, J.M., Kube, R., Wagner, W., van der Wall, B., Brooks, T.F., Burley, C.L., Beaumier, P., and Rahier, G., "Prediction and Measurement of Blade-Vortex-Interaction Loading,"First Joint CEAS/AIAA Aeroacoustics Conference (16th AIAA Aeroacoustic Conference), Munich, Germany, June 1995.

[9]Ffowcs Williams, J.E., Hawkings, D.L., "Sound Generation by Turbulence and Surfaces in Arbitrary Motion," *Philosophical Transaction of the Royal Society of London*, Series A, Vol. 264, No. 1151, May 8, 1969, pp. 321-342.

[10]Schultz, K.J., Splettstoesser, W.R., "Prediction of Helicopter Impulsive Noise using Measured Blade Pressures," 43rd Annual Forum of the American Helicopter Society, St. Louis, Mo., May, 1993.

[11]Spiegel, P., Rahier, G., Michea, B., "Blade-Vortex Interaction Noise: Prediction and Comparison with Flight and Windtunnel Tests." Eighteenth European Rotorcraft Forum, Avignon, France, Sept. 1992.

[12]Gallman, J.M., "The Validation and Application of a Rotor Acoustic Prediction Computer Program," *Proceedings of the Army Science Conference*, Durham, North Carolina, June 1990.

[13]Brentner, K.S., "Prediction of Helicopter Rotor Discrete Frequency Noise," NASA TM 87721, Oct. 1986.

[14]Brooks, T.F., Booth, E.R.,Jr., Splettstoesser, W.R., Kube, R., Niesl, G., and Steby, O., "HHC Study in the DNW to Reduce BVI Noise - An Analysis," AHS-RAes International Technical Specialists Meeting on Rotor Acoustics and Rotor Fluid Dynamics, Philadelphia, Pa., Oct. 15-17, 1991.

[15]Strawn, R., Tung, C., "The Prediction of Transonic Loading on Advancing Helicopter Rotors," NASA TM 88238, US AVSCOM TM 886-A-1, April 1986.

[16]Strawn, R.C., and Caradonna, F.X., "Conservative Full-Potential Model for Unsteady Transonic Rotor Flows," *AIAA Journal*, Vol. 25, No. 2, Feb. 1987, p.193.

[17]Caradonna, F.X., and Strawn, R.C., "An Experimental and Computational Study of Rotor-Vortex Interaction," *Vertica*, Vol. 12, No. 4, 1988, pp. 314-327.

[18]Gallman, J.M., Tung, C., Yu, Y.H., and Low, S.L., "Prediction of Blade-Vortex Interaction Noise with Applications to Higher Harmonic Control," AIAA-93-4331, 15th Aeroacoustics Conference, Long Beach, CA, Oct. 1993.

[19]Rahier, G., and Delrieux, Y., "Improvement of Helicopter Rotor Blade-Vortex Interaction Noise Prediction Using a Rotor Wake Roll-up Model," First Joint AIAA/CEAS Aeroacoustics Conference (16th AIAA Aeroacoustics Conference), Munich, Germany, June 1995.

[20]Plantin de Hugues, P., "Etude du system tourbillonnaire genere en extremite de pale d'un rotor d'helicoptere en vol stationnaire," Thesis, University of Aix-Marseille II, Marseille, France, 1991.